

Influence of excitonic effects on dynamic localization in semiconductor superlattices in combined dc and ac electric fields

Aizhen Zhang,* Lijun Yang, and M. M. Dignam

Department of Physics, Queen's University, Kingston, Ontario, Canada K7L 3N6

(Received 18 December 2002; published 23 May 2003)

We investigate the influence of excitonic effects on dynamic localization in an optically excited semiconductor superlattice in combined dc and ac electric fields. We use an excitonic basis to calculate both the quasienergy spectrum and the intraband dynamics of the system. We find that for moderate to high dc electric fields, where the Wannier-Stark ladder is only weakly disturbed by excitonic effects, the signature of dynamic localization is found in the quasienergy spectrum, the time-integrated terahertz (THz) signal, and in the decay rate of the carrier-generated THz intensity signal. However, in contrast to what is predicted by the models employing the semiconductor Bloch equations, we find that for low dc electric fields, the dynamic localization can be almost completely destroyed via excitonic effects.

DOI: 10.1103/PhysRevB.67.205318

PACS number(s): 73.21.-b, 73.23.-b, 73.63.-b, 78.67.-n

I. INTRODUCTION

Since the semiconductor superlattice (SL) was first proposed by Esaki and Tsu in 1970,¹ electronic and optical effects in superlattices have been fields of continued interest, both because of the implications for interesting device applications and for the insight into the basic principles of solid-state physics. Due to the large lattice constant and small energy-band bandwidth of this artificial structure, many effects not seen in bulk materials have been experimentally observed and many new phenomena have been predicted theoretically.

One of the most fascinating phenomena in the physics of semiconductor superlattices is the experimental realization of the long-predicted Wannier-Stark localization² and its dynamic counterpart, namely, Bloch oscillations (BO's).³ Bloch oscillations occur when a dc along-axis electric field F_0 is applied to an electron in a periodic potential (period d). The electron is then spatially localized by the dc field in a region $L = \Delta/2eF_0$ and oscillates at a frequency $\omega_B = edF_0/\hbar$, where Δ is the bandwidth. The BO's will be observed as long as $\omega_B\tau \gg 1$, where τ is the relaxation rate. Correspondingly, in a one-band model, the electronic stationary states of this system have energies $E_n = E_0 + nedF_0$, where E_0 is the energy of a particular reference state and n is an integer. Because of the equal-energy separation, they form the so-called Wannier-Stark ladder (WSL). BO's are simply the time evolution of a wave packet constructed from a linear combination of WSL states.

With the development of free-electron lasers that can be continuously tuned in the terahertz (THz) range, the dynamics of charged particles in semiconductor superlattices in time-dependent external electric fields has been a subject of intense research. In the noninteracting or single-particle picture, the evolution of electrons driven by a pure sinusoidal ac field, $F_1 \sin(\omega t)$, has been studied in great detail.⁴⁻⁸ Within the tight-binding approximation, it is found that an initially localized particle will return periodically to its initial state with the period of the ac field if the ratio Ω/ω is chosen such that $J_0(\Omega/\omega) = 0$, where

$$\Omega \equiv edF_1/\hbar \quad (1)$$

and $J_n(x)$ is the n th-order Bessel function of the first kind. This phenomenon is called dynamic localization⁹ (DL) and has been shown to be related to the collapse of the quasienergy miniband.¹⁰ This collapse has been verified experimentally for atoms in an optical lattice.¹¹ In transport measurements with photon-assisted tunneling in a Si-doped semiconductor superlattice, the appearance of absolute negative conductance has been attributed to dynamic localization.⁵

In the presence of a dc field F_0 as well as a high-frequency ac field $F_1 \sin(\omega t)$, it is found that when $edF_0 = n\hbar\omega$ —i.e., the ac field is tuned to an “ n -photon resonance” with the Wannier-Stark ladder—dynamic localization appears iff $J_n(\Omega/\omega) = 0$.^{4,12} Within the nearest-neighbor tight-binding (NNTB) approximation, the quasienergies of the Floquet states for the superlattice electrons in both dc and ac electric fields can be analytically obtained as¹³

$$\varepsilon(k) = (-1)^n J_n(\Omega/\omega) E(k), \quad (2)$$

where the zero-field band dispersion is given by the NNTB expression $E(k) = -(\Delta/2)\cos(kd)$. We can see that if Ω/ω is a zero of $J_n(x)$, then the quasienergy-quasimomentum dispersion disappears and band collapse occurs. The pure ac situation is thus seen to be the special case in which $n = 0$.

To date, most of the experiments in which the Wannier-Stark ladder and Bloch oscillations have been identified were performed in optically excited undoped semiconductor superlattices.¹⁴⁻¹⁹ In these experiments, electron-hole pair wave packets are excited in the SL via an ultrashort optical pulse. This creates well-defined wave packets. However, due to the electron-hole Coulomb interaction, the wave packets are excitonic wave packets and not simply electron wave packets. Consequently, one must treat the excitonic effects on the dynamic localization when both a dc and an ac electric field are applied in this system. This is the aim of this paper.

There are a number of approaches for treating the dynamics of electrons and holes near the semiconductor band edge

in photoexcited semiconductor superlattices. A very successful and widespread approach employs the semiconductor Bloch equations (SBE's).²⁰ They have the advantage that when used in the Hartree-Fock (HF) approximation, they are, in principle, nonperturbative in the optical field. Within a one-dimensional tight-binding model, using the SBE's, Meier *et al.*²¹ have calculated the time-integrated square of the terahertz signal generated by a photoexcited semiconductor superlattice in an applied ac electric field $F_1 \sin(\omega t)$ and predicted that the dynamic localization should be observable in the presence of the Coulomb interactions, the signature of the dynamic localization being a dip in the time-integrated THz (TITHz) signal when $J_0(\Omega/\omega)=0$. Later, again using the SBE's, Yan *et al.*²² theoretically modeled the TITHz signal in both dc and ac electric fields and found that dynamic localization still appears in the presence of the Coulomb interactions. Recently, based on SBE's, Liu and Zhu²³ have investigated the degenerate four-wave-mixing (DFWM) signals in such a system. Their calculations indicate that when dc-ac-induced dynamic localization occurs, the time-integrated DFWM signal is a maximum.

It has been pointed out by many authors,^{24–26} however, that the SBE's within the HF approximation neglect the crucial electron-hole correlations within an exciton when carried out beyond the first order in the optical field. This correlation plays a significant role in the calculation of various nonlinear signals in bulk semiconductors, quantum wells, and superlattices. This correlation is missing because these equations employ a free-electron-hole basis to perform the calculation. Therefore, when the HF factoring is performed, the correlations between the electron and hole inside the exciton are not treated correctly, resulting finally in errors even to the second order in the optical field. In particular, it has been shown²⁷ that the SBE's incorrectly predict the temporal decay of excitonic effects in the intraband polarization arising from electron-hole pairs excited by an ultrashort optical pulse in a SL. Thus, the question arises as to whether the SBE prediction of DL of excitonic wave packets is correct.

To avoid the problems encountered by the SBE's, one may either use the dynamics controlled truncation (DCT) theory²⁷ or employ an excitonic basis to treat the dynamics. When using an excitonic basis, the intraexcitonic correlations are automatically incorporated into any theory. In this paper, we examine the nature of DL of the carriers when the dynamics are treated using an excitonic basis.

The excitonic basis has been employed in a number of papers^{28–30} to investigate the intraband dynamics of coupled double quantum wells and biased semiconductor SL's (BSSL's) to second order, and to calculate the third-order DFWM signals for a single quantum well in a magnetic field. Lachaine *et al.*³⁰ have employed the excitonic basis to investigate the intraband polarization in combined dc and ac fields in cases where the dc field was much larger than the ac field. However, it has never been used, to our knowledge, to examine the dynamics of a BSSL in combined dc and ac fields where the ac field amplitude is large enough to yield DL.

In this paper, we wish to investigate the effect of the electron-hole interaction on the dynamics of electrons and holes photoexcited by ultrashort (~ 100 fs) optical pulses in

BSSL's subject to combined dc and ac electric fields. We find that for moderate to high values of the dc electric field F_0 , the signature of dynamic localization is found both in the collapse of the quasienergy band and in the appearance of a local minimum in the TITHz signal, in agreement with the above-mentioned SBE results. We also find a new purely excitonic effect in these situations: the time constant for the decay of the THz intensity signal displays a pronounced minimum when the condition for DL is reached. For small dc electric fields, however, we find that the quasienergy band generally does not collapse and the TITHz signal does not reach a minimum when Ω/ω is a root of first-order Bessel function, thereby demonstrating that dynamic localization can be destroyed via excitonic effects.

The paper is organized as follows. In Sec. II, we introduce the model and present the theory employed to calculate the quasienergy spectrum and the intraband dynamics of the system. In Sec. III, we present the numerical results and analyze the influence of the excitonic effect on the dynamic localization. Sec. IV presents a summary of our results and their implications.

II. THEORY

In this section, we present the theoretical approach that we use to calculate the quasienergy spectrum and the dynamic evolution of the intraband polarization.

In the second quantized form, the Hamiltonian of the superlattice excitons in the presence of dc, ac, and optical electric fields is given by

$$H(t) = H_0 + H_{ac}(t) + H_{op}(t). \quad (3)$$

In this expression,

$$H_0 = \sum_{\nu} E_{\nu} B_{\nu}^{\dagger} B_{\nu} \quad (4)$$

is the single-exciton Hamiltonian for superlattice excitons in the presence of a dc electric field F_0 , where B_{ν}^{\dagger} (B_{ν}) is the creation (annihilation) operator for an exciton in the *dc electric field* with internal quantum number ν and energy E_{ν} . The term

$$H_{ac}(t) \equiv -\mathbf{V} \mathbf{E}_{ac}(t) \cdot \mathbf{P}_{intra} \quad (5)$$

is the interaction Hamiltonian between the ac field $\mathbf{E}_{ac}(t)$, and the excitons, where \mathbf{P}_{intra} is the *intraband* polarization defined by

$$\mathbf{P}_{intra} = \frac{1}{V} \sum_{\nu\mu} \mathbf{G}_{\nu\mu} B_{\nu}^{\dagger} B_{\mu}. \quad (6)$$

In this expression, $\mathbf{G}_{\nu\mu}$ is the *intraband* dipole matrix element between two excitonic states $|\psi^{\nu}\rangle$ and $|\psi^{\mu}\rangle$, and is given by

$$\mathbf{G}_{\nu\mu} = \langle \psi^{\nu} | -e(\mathbf{r}_e - \mathbf{r}_h) | \psi^{\mu} \rangle. \quad (7)$$

Finally, the last term in $H(t)$ is

$$H_{op}(t) \equiv -\mathbf{V} \mathbf{E}_{op}(t) \cdot \mathbf{P}_{inter}, \quad (8)$$

which is the interaction Hamiltonian between the optical field $\mathbf{E}_{op}(t)$ and the excitons, where \mathbf{P}_{inter} is the *interband* polarization defined by

$$\mathbf{P}_{inter} = \frac{1}{V} \sum_{\nu} [\mathbf{M}_{\nu} B_{\nu}^{\dagger} + \mathbf{M}_{\nu}^{*} B_{\nu}]. \quad (9)$$

The *interband* dipole matrix element of the ν th excitonic state is given by

$$\mathbf{M}_{\nu} = \mathbf{M}_0 \sqrt{AN_z} \int dz \psi^{\nu*}(z, z, 0), \quad (10)$$

where \mathbf{M}_0 is the bulk interband dipole matrix element, A is the transverse area, ψ^{ν} is the ν th SL exciton eigenstate in presence of the dc electric field, and N_z is the number of superlattice sites.

We consider excitation via ultrashort Gaussian optical pulses with central frequency ω_c and duration τ_p . Hence, the optical field is given by

$$\mathbf{E}_{opt} = \mathbf{A}_0 e^{-(t/\tau_p)^2} e^{-i\omega_c t} + \text{c.c.} \quad (11)$$

In writing the full Hamiltonian, we have assumed that the exciton density is low enough so that we can neglect the exciton-exciton interactions, and, in what follows, we will similarly neglect phase-space filling and treat the excitons as bosons.³¹ Both assumptions are rigorously valid to second order in the optical field.

In order to proceed with the calculations, we must determine the superlattice excitonic states in the presence of the dc electric field. This is accomplished by using the two-well excitonic method of Dignam and Sipe.³² To determine which excitonic states to include in the basis, we note first that only excitons with zero center-of-mass momentum will be optically excited. Second, if the exciting laser pulse has an energy spectrum centered below the $n=0$ WSL state, it has been shown²⁸ that predominantly $1s$ -like excitons are created and the excitonic states with excited in-plane motion can be neglected. Thus, in this work we will only consider the $1s$ -like excitonic states with zero center-of-mass momentum.

The first way in which we examine the phenomenon of dynamic localization in the photoexcited superlattices is by determining the quasienergy spectra of the excitons in the presence of the ac electric field. The SL is excited by an ultrashort (~ 100 fs) optical pulse. Then, once the pulse has passed, the Hamiltonian is given simply by

$$H'(t) = H_0 + H_{ac}(t). \quad (12)$$

We take the ac field to be given by

$$\mathbf{E}_{ac}(t) = F_1 \sin(\omega t) = \frac{\hbar\Omega}{ed} \sin(\omega t), \quad (13)$$

where $\hbar\omega$ is chosen to be equal to the WSL spacing for the given dc field, i.e., $\omega = \omega_B$. Thus, the Hamiltonian $H'(t)$ is periodic with period $T = 2\pi/\omega$.

We can make use of the periodicity of the exciton Hamiltonian $H'(t)$, and the calculated excitonic energy levels and

eigenstates to numerically calculate the quasienergy spectrum. For a numerical calculation of the quasienergies, it is convenient to introduce the time evolution operator $U(t)$, that satisfies the equation

$$i\hbar \frac{\partial}{\partial t} U(t) = H'(t) U(t), \quad (14)$$

with the initial condition $U(0) = 1$. Within the framework of the Floquet formalism,³³ we obtain

$$[U(T) - e^{-i\varepsilon T}] |\psi(0)\rangle = 0, \quad (15)$$

where ε is the quasienergy and $|\psi(0)\rangle$ is the initial state of the Floquet state. Thus, the quasienergies and Floquet states can be determined directly by numerically integrating Eq. (14) over one period and diagonalizing $U(T)$ in the basis of excitonic eigenstates.

We now turn to the calculation of the intraband polarization created by the optical pulse. Using the full Hamiltonian (3), the equations of motion for the expectation values of the interband and intraband correlation functions to the second order in the optical field are³⁰

$$i\hbar \frac{d\langle B_{\nu}^{\dagger} \rangle}{dt} = - \left(E_{\nu} + \frac{i\hbar}{T_{2inter}} \right) \langle B_{\nu}^{\dagger} \rangle + \mathbf{E}_{opt}(t) \cdot \mathbf{M}_{\nu}^{*} + \mathbf{E}_{ac}(t) \cdot \sum_{\beta} \mathbf{G}_{\beta\nu} \langle B_{\beta}^{\dagger} \rangle, \quad (16)$$

$$i\hbar \frac{d\langle B_{\mu}^{\dagger} B_{\nu} \rangle}{dt} = \left(E_{\nu} - E_{\mu} - \frac{i\hbar}{T_{\mu\nu}} \right) \langle B_{\mu}^{\dagger} B_{\nu} \rangle + \mathbf{E}_{opt}(t) \cdot [\mathbf{M}_{\mu}^{*} \langle B_{\nu} \rangle - \mathbf{M}_{\nu} \langle B_{\mu}^{\dagger} \rangle] + \mathbf{E}_{ac}(t) \cdot \sum_{\beta} [\mathbf{G}_{\beta\mu} \langle B_{\beta}^{\dagger} B_{\nu} \rangle - \mathbf{G}_{\nu\beta} \langle B_{\mu}^{\dagger} B_{\beta} \rangle], \quad (17)$$

where T_{2inter} is the interband dephasing time, and $T_{\mu\nu}$ is defined such that $T_{\mu\nu} = T_1$ (excitonic population decay time) if $\mu = \nu$ and $T_{\mu\nu} = T_{2intra}$ if $\mu \neq \nu$, where T_{2intra} is the intraband dephasing time.

Once Eqs. (16) and (17) are solved, we obtain the intraband polarization given by the expectation value of Eq. (6). For the experiments of interest, the emitted radiation is at THz frequencies. The *intensity* of the emitted THz signal is given by

$$I_{THz}(t) \propto \left\langle \left[\frac{d^2}{dt^2} P_{intra}(t) \right]^2 \right\rangle_T, \quad (18)$$

where the angular brackets indicate a time average over times of the order of the BO period. The TITHz signal is simply obtained from the time-integral of $I_{THz}(t)$ over all time.

III. RESULTS

In order to demonstrate the effects of the electron-hole correlation (i.e., excitonic effects) on the DL in a biased semiconductor superlattice, we consider a GaAs/Ga_{0.7}Al_{0.3}As

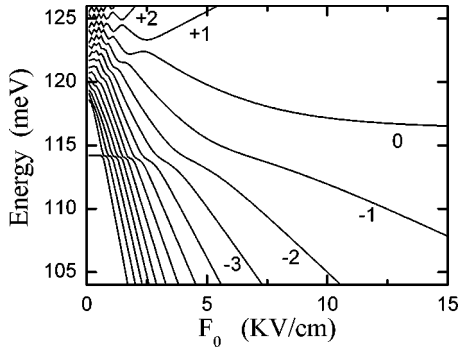


FIG. 1. The exciton energy levels (relative to the band gap of bulk GaAs) as a function of the dc electric field F_0 for the 45/45 superlattice discussed in the text. The numbers beside each curve gives the quantum number ν for the excitonic state.

superlattice structure with a 45 Å well width and a 45 Å barrier width. The parameters used in the calculation are given in Ref. 32. The calculations are performed using 25 basis states as we find that there is no change in the calculated dynamic results with an increase in the basis size beyond this. The ability to truncate the basis in this way is due to the fact that the only excitonic WSL states that will be optically excited are those for which the electron-hole overlap is appreciable.³² The resulting combined electron-hole miniband has a width of $\Delta \approx 10$ meV. This superlattice was chosen because it is well described by a nearest-neighbor tight-binding Hamiltonian, and hence should exhibit DL when a sinusoidal field is applied. The calculations are performed for dc fields of $F_0 = 3$ kV/cm and $F_0 = 10$ kV/cm, for which $\omega = \omega_B$ is $4.1 \times 10^{12} \text{ s}^{-1}$ and $1.37 \times 10^{13} \text{ s}^{-1}$, respectively.

We begin by plotting in Fig. 1 the 1s excitonic WSL energies as a function of dc electric field F_0 , using the method of Dignam and Sipe.³² The energy levels are labeled by the index ν that corresponds to the free-particle WSL index n when the field is relatively high. More exactly, the expectation value of the electron-hole separation is given approximately by νd in the high-field limit. We can see that the excitonic energy levels differ substantially from those of the single-particle Stark ladder levels, which would appear as a set of straight lines with energy separations of $eF_0 d$, all converging to a point at $F_0 = 0$. Because the effect of the electron-hole Coulomb interaction on the energy is different for the different states—i.e., the exciton binding energies for states with different ν are different—the separation $E_{\nu+1}(F) - E_{\nu}(F)$ between adjacent energy levels is not $eF_0 d$, but is dependent on ν . In addition, in contrast to the noninteracting picture, the intraband dipole matrix elements $G_{\nu, \nu+\mu}$ and $G_{\nu, \nu-\mu}$ (not shown) are not equal and depend on ν . These effects have already been discussed in detail.³⁰ Given that the excitonic WSL energies differ considerably from the free-electron-hole WSL, we expect that in many cases, DL will be altered considerably by excitonic effects, in contrast to the results of SBE calculations.

We begin our examination of excitonic effects on DL by plotting in Fig. 2 the quasienergy spectrum of the system. Figure 2(a) shows the quasienergy band in the noninteracting

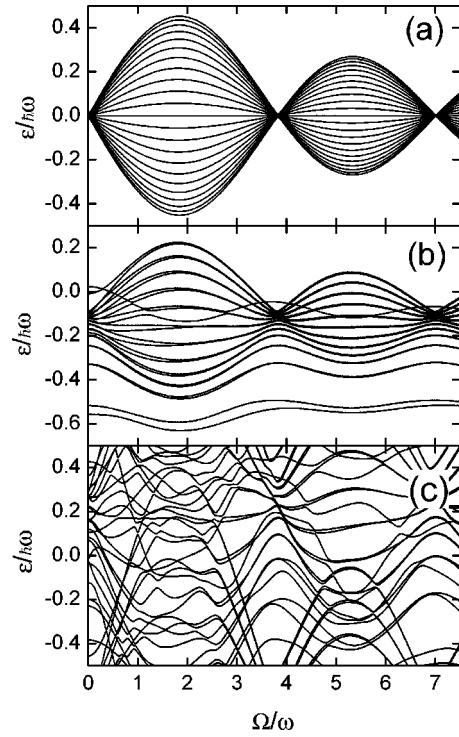


FIG. 2. The quasienergy ε as a function of Ω/ω for (a) the single-particle (noninteracting) picture, (b) the excitonic system with $F_0 = 10$ kV/cm, and (c) the excitonic system with $F_0 = 3$ kV/cm.

electron-hole approximation, where a total band collapse can be seen at DL points, i.e., where $J_1(\Omega/\omega) = 0$ ($\Omega/\omega = 0, 3.8317, 7.0156, \dots$). For future reference, we define Ω_o to denote the first DL point: $\Omega_o \equiv 3.8317\omega$.

Figures 2(b) and 2(c), respectively, show the quasienergy bands as a function of Ω/ω for dc electric fields of $F_0 = 10$ kV/cm and $F_0 = 3$ kV/cm. We note that in both cases, because of the influence of excitonic effects, no total band collapse occurs. However, for a field of $F_0 = 10$ kV/cm, the signature of band collapse is clearly seen when $\Omega = \Omega_o$. For the low dc field of $F_0 = 3$ kV/cm, however, the excitonic effect so strongly modifies the noninteracting quasienergy spectrum that there is no discernible signature of band collapse for any values of Ω/ω . Thus, it appears that the electron-hole interaction has effectively destroyed DL for a dc field of 3 kV/cm. We find, more generally, that DL is destroyed at any field strengths where the excitonic effect has strongly disturbed the WSL spacings and intraband dipole matrix elements. Typically, this occurs for fields for which the excitonic binding energy for the $\nu = 0$ state is larger than the WSL ladder spacing. Since the binding energy is typically of the order of 8 meV, DL will only be observed when $edF_0 \geq 8$ meV. This suggests that DL may not be observed in pure ac fields. However, when $F_0 = 0$ the unbound excitons play a much larger role and may dominate the dynamics. Thus, to treat such a system accurately, it would be necessary to include the unbound excitonic states, which have not been included in our basis.

The quasienergy bands cannot be directly observed experimentally. For the experimental signature of DL, we turn

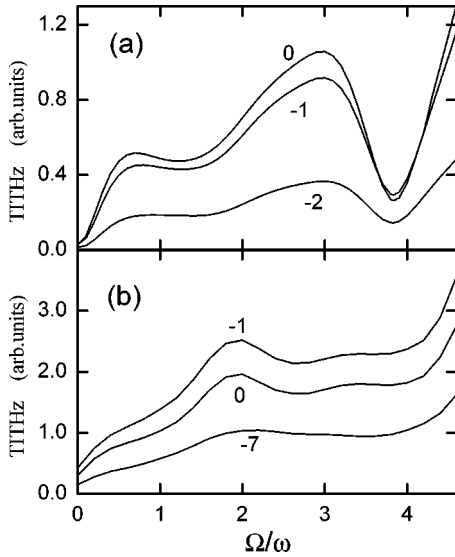


FIG. 3. The time-integrated carrier-generated THz signal as a function of Ω/ω for (a) $F_0=10$ kV/cm and (b) $F_0=3$ kV/cm for three different central laser frequencies. The laser frequency in all cases is given by $\omega_c=E_\nu/\hbar$, where the index ν for each curve is given beside the curve.

to the THz signal generated by the photoexcited oscillating excitonic wave packets. We take the temporal full width half maximum (FWHM) of the optical pulse to be 118 fs (spectral FWHM of 15.5 meV). The laser central frequency is chosen in all cases such that $\hbar\omega_c \leq E_0$. With this restriction, the photoexcited $1s$ exciton population is considerably larger than the population of unbound electron-hole pairs.²⁸ The TITHz signal (normalized to the excited excitonic population) is plotted in Fig. 3 as a function of Ω/ω for four different central laser frequencies ω_c . In the calculations, we employ an interband dephasing time of 0.52 ps and intraband dephasing time 1.04 ps, in agreement with experiment,³⁴ and neglect the population decay ($T_1=\infty$). The results for dc fields of $F_0=10$ kV/cm and $F_0=3$ kV/cm are shown in Figs. 3(a) and 3(b), respectively. We first note that there is qualitatively little dependence on the central laser frequency. We generally find this to be the case as long as $|\hbar\omega_c - E_0|$ is small enough such that the photoexcited states still have a strong excitonic character. As we expect from the quasienergy spectra, the TITHz signal reaches a minimum when $\Omega = \Omega_o$ for the $F_0=10$ kV/cm case for all three different excitation conditions, while no such minimum appears in the $F_0=3$ kV/cm case. This demonstrates first that excitonic DL can be observed for large dc electric fields. Second, it verifies the quasienergy results: dynamic localization can be destroyed for any dc electric field for which the excitonic effects strongly perturb the WSL.

The excitonic effects do more than suppress DL, however. They also qualitatively modify the temporal behavior of the THz signal even in those cases where DL is observed. To demonstrate this, we plot in Fig. 4 the time evolution of the square of the carrier-generated THz radiation field for $F_0=10$ kV/cm for various values of Ω near Ω_o . To aid in the analysis, we averaged the THz signals over a time interval of

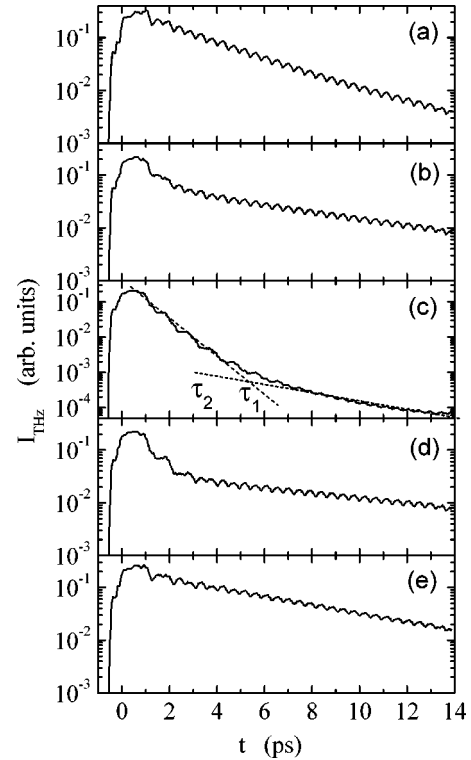


FIG. 4. The time evolution of the carrier-generated THz intensity signal $I_{THz}(t)$ on a log scale for different Ω/ω : (a) $\Omega/\omega=3$, (b) $\Omega/\omega=3.5$, (c) $\Omega/\omega=3.8317$, (d) $\Omega/\omega=4.1$, and (e) $\Omega/\omega=4.5$. The dashed lines in (c) and (d) indicate the exponential decay associated with the two different time constants.

1 ps to remove the rapid oscillations; this time-averaged quantity is thus the THz intensity. We find that when we are sufficiently far from the condition for DL [Figs. 4(a) and 4(e)], the THz intensity dies out exponentially with a single time constant τ_1 that is much greater than the intensity decay rate of $\frac{1}{2}T_{2intra}$ that one would naturally expect. However, when Ω/ω is close to the value for DL [Figs. 4(b)–4(d)], the THz intensity is seen to decay with two very different time constants, such that the intensity is given approximately by $I(t)=I_1e^{-t/\tau_1}+I_2e^{-t/\tau_2}$, where $I_2 \ll I_1$ and $\tau_2 \gg \tau_1$. Most importantly, the initial decay constant τ_1 is much smaller than what we obtained when we were far from the condition for DL [Figs. 4(a) and 4(e)]. To quantify the dependence of the THz intensity signal decay time on the ac field strength, we plot in Fig. 5 the decay constant τ_1 as a function of Ω/ω . As noted above, when Ω is far from Ω_o , the decay time is much longer than the expected dephasing time of $T_{2intra}/2$, while at the DL point the decay time is approximately equal to (but slightly larger than) $T_{2intra}/2$. Thus, by measuring the time constant τ_1 , one should see a clear signature of DL.

The source of the very long decay time τ_1 when we are far from the DL condition is entirely excitonic in nature. An ac field cannot “drive,” the amplitude of the BO of noninteracting particles because the probability of making an up transition ($n \rightarrow n+1$) in the WSL is equal to that of making a down transition ($n \rightarrow n-1$). However, as was first pointed out by Lachaine *et al.*³⁰ by producing unequal WSL spacings and intraband dipole matrix elements, excitonic effects de-

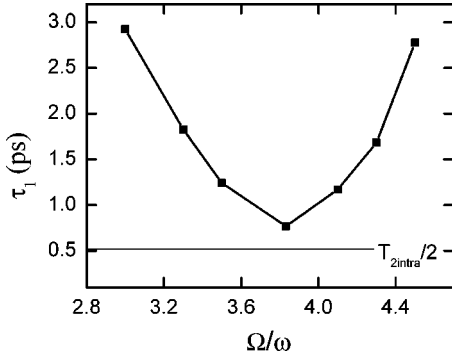


FIG. 5. The initial decay constant τ_1 for the THz intensity as a function of Ω/ω . Also shown in the plot (thin line) is the expected intensity decay time of $T_{intra}/2$ for undriven (freely-decaying) BO.

stroy this up-down symmetry. Thus, an ac electric field is able to drive the amplitude of *excitonic* Bloch oscillations. This driving of the oscillation amplitude is what is responsible for the very long τ_1 when we are far from the condition for DL. In addition, as long as the carriers continue to oscillate, the ac field can do work on the excitons (positive or negative work depending on the relative phase) by changing the average separation of the electrons and holes in the z direction. This effect is analogous to the Shapiro effect in Josephson junctions.³⁵ This manifests itself as a steady increase in the intraband polarization with time.

The two effects of the driving of the oscillation amplitude and the driving of the time-averaged electron-hole separation are found to be intimately connected; you can only drive the time-averaged separation while the oscillation amplitude persists. This is best seen by examining the expectation value of the intraband polarization. In Fig. 6, we plot the intraband polarization for $\Omega = \Omega_o$ (DL) and $\Omega/\omega = 3.0$ (far from DL). As can be seen, when $\Omega/\omega = 3.0$, the oscillations in P_{intra} persist for times much greater than T_{2intra} , and the average value of P_{intra} increases rapidly and steadily out beyond a time of 14 ps. In clear contrast to this, when $\Omega = \Omega_o$, the oscillations die out at a time that is only slightly larger than T_{2intra} , while the average value of P_{intra} increases appreciably only for $t \lesssim 1.5T_{2intra}$ and after that “saturates” to an approximately constant value. Thus, it appears that when we

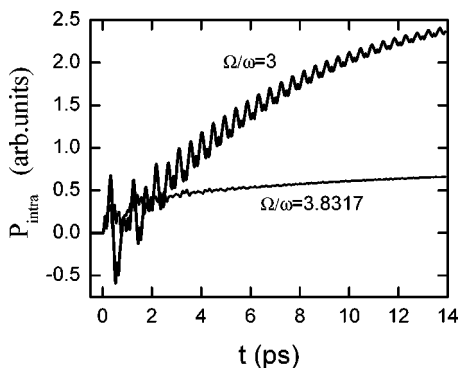


FIG. 6. The intraband polarization as a function of time for $\Omega/\omega = 3.0$ (bold line) and $\Omega = \Omega_o$ (thin line) for a dc field of $F_0 = 10$ kV/cm.

are near the condition for DL, the ac field is ineffective in driving the BO amplitude or in changing the average intraband polarization of the carriers.

The physics behind the inability of the ac field to drive the BO when we are at the condition for DL is most easily explained by examining the electron dynamics in a rectangular-wave ac field in the absence of dephasing. Consider a periodic, rectangular field of the form

$$E(t) = \begin{cases} E_1 & 0 \leq t < T_1 \\ -E_2 & T_1 \leq t < T_1 + T_2, \end{cases} \quad (19)$$

where $E(t)$ is periodic with period T and $T \equiv T_1 + T_2$. Depending on the values for E_1 and E_2 , this may be a pure ac field or a field with ac and dc components. As has been pointed out by a number of authors,^{6,36} for noninteracting particles, DL will occur if an integer number n_1 of BO occurs during the time $0 \leq t < T_1$ and an integer number n_2 of BO occurs during the second half of the period, $T_1 \leq t < T_1 + T_2$. This requires that $E_1 = n_1 2\pi\hbar/(edT_1)$ and $E_2 = n_2 2\pi\hbar/(edT_2)$. Under these conditions, the wave packet clearly returns to its initial state after one period and hence DL is achieved. Now, because the wave packet is periodic in time, it is clear that there can be no net work done on the electrons during the period of the rectangular field, i.e., there can be no Shapiro effect. In fact, because the field only changes at times when the electron is in the same state, for the most part the field effectively acts as if it is a pure dc field. Now, if we consider excitonic dynamics in such a field, it is easily seen that if we choose fields E_1 and E_2 such that the exciton wave packet is essentially back in its initial state before the field changes sign at times T_1 and T , then the excitons will act as if they are effectively in a dc electric field. If this is the case, then there will be no driving of the BO, because BO cannot be “driven” by a dc electric field. Thus, there will be no Shapiro effect and the BO amplitude will not be driven.

Because the excitonic BO contains several oscillation frequencies, it will, in general, be impossible to *exactly* satisfy the conditions required to change field sign only when the wave packet is back to its initial state. However, because the frequencies are not very different, the condition can nearly be met. Thus, there is only a relatively weak Shapiro effect (slow rise in the average polarization in Fig. 6) and the BO only persists for times slightly larger than T_{2intra} (see Fig. 5). For clarity, the physical argument presented here is for the case of a rectangular wave. However, the physics behind the argument is essentially the same for the sinusoidal field used in the calculations. In either case, the general physical picture is that *an applied ac field will not drive BO when the field amplitude is such that the conditions for DL are met.*

IV. CONCLUSIONS

In this paper, we used an excitonic basis to investigate the dynamics of optically excited semiconductor superlattices in combined dc and ac electric fields. We found that signatures of DL are evident in the THz signal and in the decay times of the THz radiation as long as the dc electric field is not too

small. However, in low dc electric fields, where the excitonic binding energies are comparable or larger than the WSL energy spacings, the excitonic effects effectively destroy dynamic localization.

Finally, we discuss the feasibility of the experiments proposed in this paper. All the experimental elements discussed in this paper are readily available: the production of 100-fs optical pulses are routine, as are the methods for time-resolved measurements of THz electric fields³⁸ using photoconducting antennas. The most difficult aspect of these experiments is likely to be the generation of high-intensity THz fields. However, using a free-electron laser, the ac frequencies and field strengths discussed in this work can be experi-

mentally achieved.^{5,37} Thus, experiments measuring the time-integrated and time-resolved THz emission from SL's are feasible and would provide a clear demonstration of DL and its destruction via excitonic effects at low dc electric fields. Furthermore, they would provide direct evidence of the driving of BO via ac fields when one is far from the condition for DL.

ACKNOWLEDGMENTS

This work was supported in part by PREA and by the Natural Sciences and Engineering Research Council of Canada.

*Permanent address: Department of Physics and Institute of Theoretical Physics, Shanxi University, Taiyuan 030006, People's Republic of China.

¹L. Esaki and R. Tsu, IBM J. Res. Dev. **14**, 61 (1970).

²G.H. Wannier, Phys. Rev. **117**, 432 (1960).

³F. Bloch, Z. Phys. **52**, 555 (1928).

⁴X.-G. Zhao, Phys. Lett. A **167**, 291 (1992); J. Phys.: Condens. Matter **6**, 2751 (1994).

⁵B.J. Keay, S. Zeuner, S.J. Allen, K.D. Maranowski, A.C. Gossard, U. Bhattacharya, and M.J.W. Rodwell, Phys. Rev. Lett. **75**, 4102 (1995).

⁶M.M. Dignam and C.M. de Sterke, Phys. Rev. Lett. **88**, 046806 (2002).

⁷X.-G. Zhao, G.A. Georgakis, and Q. Niu, Phys. Rev. B **54**, R5235 (1996).

⁸A.W. Ghosh, A.V. Kuznetsov, and J.W. Wilkins, Phys. Rev. Lett. **79**, 3494 (1997).

⁹X.-G. Zhao, Phys. Lett. A **155**, 299 (1991); D.H. Dunlap and V.M. Kenkre, Phys. Rev. B **34**, 3625 (1986).

¹⁰M. Holthaus, Phys. Rev. Lett. **69**, 351 (1992); Z. Phys. B: Condens. Matter **89**, 251 (1992).

¹¹K.W. Madison, M.C. Fischer, R.B. Diener, Q. Niu, and M.G. Raizen, Phys. Rev. Lett. **81**, 5093 (1998).

¹²X.-G. Zhao, R. Jahnke, and Q. Niu, Phys. Lett. A **202**, 297 (1995).

¹³M. Holthaus and D. Hone, Phys. Rev. B **47**, 6499 (1993); J. Zak, Phys. Rev. Lett. **71**, 2623 (1993).

¹⁴C. Waschke, H.G. Roskos, R. Schwedler, K. Leo, H. Kurz, and K. Köhler, Phys. Rev. Lett. **70**, 3319 (1993).

¹⁵E.E. Mendez, F. Agullo-Rueda, and J.M. Hong, Phys. Rev. Lett. **60**, 2426 (1988).

¹⁶P. Voisin, J. Bleuse, C. Bouche, S. Gaillard, C. Alibert, and A. Regreny, Phys. Rev. Lett. **61**, 1639 (1988).

¹⁷P. Leisching, P. Haring Bolivar, W. Beck, Y. Dhaibi, F. Brügge-mann, R. Schwedler, H. Kurz, K. Leo, and K. Köhler, Phys. Rev. B **50**, 14389 (1994).

¹⁸V.G. Lyssenko, G. Valusis, F. Löser, T. Hasche, K. Leo, M.M. Dignam, and K. Köhler, Phys. Rev. Lett. **79**, 301 (1997).

¹⁹J. Feldmann, K. Leo, J. Shah, D.A.B. Miller, J.E. Cunningham, T. Meier, G. von Plessen, A. Schulze, P. Thomas, and S. Schmitt-Rink, Phys. Rev. B **46**, 7252 (1992).

²⁰H. Haug and S. W. Koch, *Quantum Theory of the Optical and Electronic Properties of Semiconductors*, 3rd ed. (World Scien-

tific, Singapore, 1994).

²¹T. Meier, G. von Plessen, P. Thomas, and S.W. Koch, Phys. Rev. B **51**, 14 490 (1995).

²²W.X. Yan, S.Q. Bao, X.-G. Zhao, and J.-Q. Liang, Phys. Rev. B **61**, 7269 (2000).

²³Ren-Bao Liu and Bang-Fen Zhu, Phys. Rev. B **59**, 5759 (1999).

²⁴G. Bartels, G.C. Cho, T. Dekorsy, H. Kurz, A. Stahl, and K. Köhler, Phys. Rev. B **55**, 16 404 (1997).

²⁵Margaret Hawton and Delene Nelson, Phys. Rev. B **57**, 4000 (1998).

²⁶W. Schäfer, D.S. Kim, J. Shah, T.C. Damen, J.E. Cunningham, K.W. Goossen, L.N. Pfeiffer, and K. Köhler, Phys. Rev. B **53**, 16 429 (1998).

²⁷V.M. Axt, G. Bartels, and A. Stahl, Phys. Rev. Lett. **76**, 2543 (1996).

²⁸M. Dignam, J.E. Sipe, and J. Shah, Phys. Rev. B **49**, 10502 (1994).

²⁹Wei Min Zhang, Torsten Meier, Vladimir Chernyak, and Shaul Mukamel, Phys. Rev. B **60**, 2599 (1999).

³⁰J.M. Lachaine, Margaret Hawton, J.E. Sipe, and M.M. Dignam, Phys. Rev. B **62**, R4829 (2000).

³¹For a more complete treatment of the Hamiltonian beyond the low-density limit, see M. M. Dignam and M. Hawton, Phys. Rev. B **67**, 035329 (2003).

³²M.M. Dignam and J.E. Sipe, Phys. Rev. Lett. **64**, 1797 (1990); Phys. Rev. B **43**, 4097 (1991).

³³K.F. Milfeld and R.E. Wyatt, Phys. Rev. A **27**, 72 (1983).

³⁴P.H. Bolivar, F. Wolter, A. Müller, H.G. Roskos, H. Kurz, and K. Köhler, Phys. Rev. Lett. **78**, 2232 (1997).

³⁵F. Löser, M.M. Dignam, Yu.A. Kosevich, K. Köhler, and K. Leo, Phys. Rev. Lett. **85**, 4763 (2000).

³⁶M.J. Zhu, X.-G. Zhao, and Q. Niu, J. Phys.: Condens. Matter **11**, 4527 (1999).

³⁷P.S.S. Guimaraes, B.J. Keay, J.P. Kaminski, S.J. Allen, P.F. Hopkins, A.C. Gossard, L.T. Florez, and J.P. Harbison, Phys. Rev. Lett. **70**, 3792 (1993); K. Unterrainer, B.J. Keay, M.C. Wanke, S.J. Allen, D. Leonard, G. Medeiros-Ribeiro, U. Bhattacharya, and M.J.W. Rodwell, *ibid.* **76**, 2973 (1996); S. Zeuner, B.J. Keay, S.J. Allen, K.D. Maranowski, A.C. Gossard, U. Bhattacharya, and M.J.W. Rodwell, Phys. Rev. B **53**, R1717 (1996).

³⁸Jagdeep Shah, *Ultrafast Spectroscopy of Semiconductors and Semiconductor Nanostructures* (Springer-Verlag, New York, 1996), Sec. 2.12.